

# Identification and kinetic characterization of a novel superoxide dismutase from *Avicennia marina*: An antioxidant enzyme with unique features



Farrokhzad Zeinali<sup>a</sup>, Ahmad Homaei<sup>b,\*</sup>, Ehsan Kamrani<sup>a,c</sup>

<sup>a</sup> Department of Marine Biology, Faculty of Sciences, University of Hormozgan, Bandar Abbas, Iran

<sup>b</sup> Department of Biochemistry, Faculty of Sciences, University of Hormozgan, Bandar Abbas, Iran

<sup>c</sup> Fisheries Department, Faculty of Marine Sciences, University of Hormozgan, Bandar Abbas, Iran

## ARTICLE INFO

### Article history:

Received 5 July 2016

Received in revised form 3 July 2017

Accepted 9 July 2017

Available online 16 July 2017

### Keywords:

Superoxide dismutase

*Avicennia marina*

Antioxidant enzyme

Persian Gulf

## ABSTRACT

A novel Cu/Zn-superoxide dismutase was extracted from *Avicennia marina* and purified. The sample was collected from Khamir port located in the north shore of Persian Gulf. The purification procedure comprised of  $(\text{NH}_4)_2\text{SO}_4$  precipitation followed by CM-Sephadex C-50 and DEAE-Sepharose chromatography, and gel filtration chromatography (Sephadex G-75). The enzyme with a characteristic molecular weight of 31 kDa, measured by SDS-page, showed its highest catalytic efficiency at pH 8.0 and 50 °C. Its activity was greatly inhibited by cyanide and hydrogen peroxide. The pH profile showed that the enzyme could maintain most of its activity at pH values ranging from 5 to 10. The temperature profile of this enzyme showed a broad range of activity compared with other superoxide dismutases.

Catalytic hydrolysis rate followed Michaelis–Menten equation. The values of  $k_{cat}$  and  $K_m$  were obtained from Michaelis–Menten plot as 107000 s<sup>-1</sup> and 11.5 μmol respectively. The evidences from kinetic and thermodynamic parameters suggest that *Avicennia marina* superoxide dismutase (AmSOD) can be used as a suitable enzyme for biotechnological and pharmacological applications.

© 2017 Elsevier B.V. All rights reserved.

## 1. Introduction

Mangroves are forest community within the intertidal region of tropical and subtropical areas [1,2], and have even expanded to some temperate locales [3]. They provide various ecological and economical ecosystem services contributing to coastal erosion protection, water filtration, provision of areas for fish and shrimp breeding, provision of building material and medicinal ingredients, and the attraction of tourists, amongst many other factors [4]. Iran has the highest acreage of natural mangrove forest ranking 43rd in the world and 10th in Asia. Mangrove forests on the southern coast of Iran, “The Hara forests”, cover several locations between the 25°11' and 27°52' parallels. Mangrove growth in Iran consists of only two species of trees, ‘Hara’ (*Avicennia marina*) and ‘Chandal’ (*Rhizophora mucronata*), with *A. marina* scrub being the most prolific, contributing over 90% of the Oman Sea and Persian Gulf's

mangrove habitats [1]. Plants in the environment are exposed to a range of abiotic stresses like osmotic, salinity, temperature and heavy metal toxicity which may affect their growth and other physiological processes [5].

Reactive oxygen species (ROS) are produced during normal aerobic respiration processes. Their level is controlled by a natural balance between ROS production antioxidant system [6]. Superoxide dismutases (SOD; EC1.15.1.1) are the first and most important of antioxidant metalloenzymes, dismutation  $\text{O}_2^-$  into  $\text{H}_2\text{O}_2$  and  $\text{O}_2$  [7] SODs are according to the type of metal bound at their active site: Cu/Zn-SOD, Mn-SOD, Fe-SOD, and Ni-SOD [8].

Halophytic plants like mangroves have been reported to have a high level of SOD activity, which plays a major role in defending the mangrove species against severe abiotic stresses [9].

SODs have been extracted from various species including animal plasma or plant cells. Green plant and macroalgae may also be suitable sources for extracting the enzyme [7]. A marine enzyme may be a unique protein molecule not found in any terrestrial organism or it may be a known enzyme from a terrestrial source with novel properties [10–13]. Considering the fact that *Avicennia marina* is exclusively found in Persian Gulf and the fact that SOD, responsible for its unique antioxidant behavior, has not been studied so

\* Corresponding author at: Department of Biochemistry, Faculty of Sciences, University of Hormozgan, Bandar Abbas, P.O. Box 3995, Iran.

E-mail addresses: [a.homaei@hormozgan.ac.ir](mailto:a.homaei@hormozgan.ac.ir), [\(A. Homaei\).](mailto:a.homaei@gmail.com)

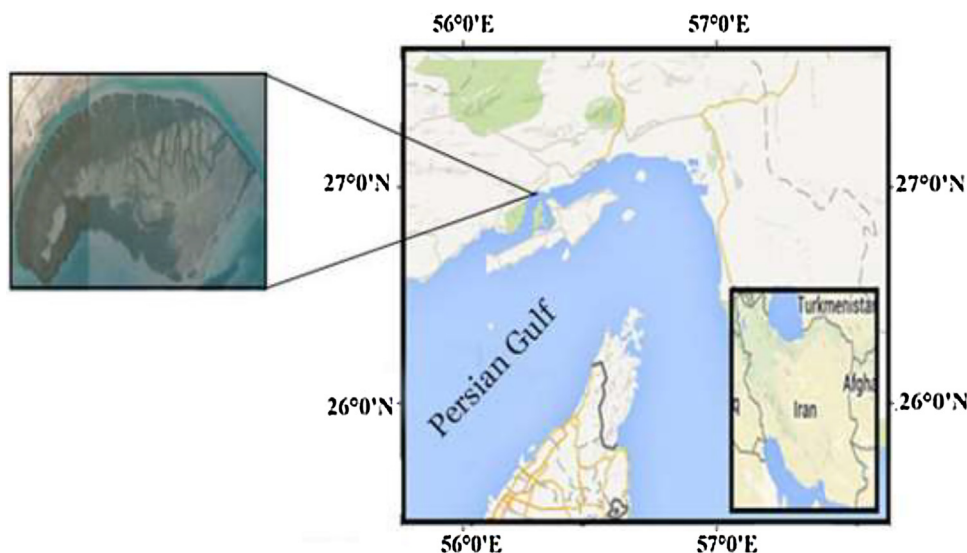


**Fig. 1.** The place of origin of the *Avecina marina* in Persian Gulf. The samples come from port of Khamir in the north shore of Persian Gulf, Hormozgan province, Iran.

far, we aimed to extract, purify, identify and characterize this novel superoxide dismutase. The specific information obtained from this research could open a way to further characterize the enzyme and design its various industrial and medical applications.

## 2. Materials and methods

### 2.1. Specimen collection and crude enzyme extraction

Three samples, approximately 20 leaves of *A. marina*, were collected from port of Khamir in the north shore of Persian Gulf, Hormozgan province, Iran (Fig. 1). Each sample was obtained from 5 to 10 trees, each taller than 3 m with girth at breast height >20 cm, and of similar health conditions. The samples were washed immediately, blotted on filter paper, frozen and transported to our enzymology laboratory in Hormozgan University, Bandar Abbas. The frozen samples were then stored at -4 °C until used. Fresh leaves (5 g) were ground in porcelain mortar with liquid nitrogen and the leaf paste was squeezed. Enzyme was extracted from the tissue powder homogenized in 10 ml of 50 mM Tris-HCl buffer, pH 7.5 and centrifuged at 15,000g for 20 min. The homogenates were centrifuged and the precipitates removed.

### 2.2. Isolation and purification

#### 2.2.1. Ammonium sulfate precipitation

The supernatant was slowly brought to 20% saturation with solid ammonium sulfate under stirring at 4 °C. The solution was centrifuged at 12,000g for 20 min and the supernatant fraction was brought to 85% saturation with solid ammonium sulfate and stirred at 4 °C. After centrifugation, the precipitate was collected and dissolved in minimal amount of Tris buffer, pH 7.5 and dialyzed against the same buffer for 24 h at 4 °C, changing dialysis buffer every 8 h.

#### 2.2.2. Cation-exchange chromatography

The dialyzed sample was subjected to cation-exchange chromatography, using a CM-Sephadex C-50 column, previously equilibrated with 50 mM phosphate buffer pH 7.5. The column was washed with the same buffer until no protein was detected in the eluent. It was then eluted using a gradient of 0–1 M NaCl in the same buffer with a flow rate of 0.5 ml/min and 2.0 ml fractions were collected. To determine the total protein content of each fraction, the absorbance at 280 nm was measured by UV-vis spectrophotome-

ter. The active fractions from this and subsequent chromatography fractions were assayed using pyrogallol as a substrate.

#### 2.2.3. Anion-exchange chromatography

Fractions with SOD activity were pooled and applied to a DEAE –Sephadex fast flow column, pre-equilibrated with 50 mM phosphate buffer at pH 7.5. The column was washed with the same buffer until no protein was detected in the eluent (lack of absorption at 280 nm). It was then eluted on a gradient of 0–1 M NaCl in the same buffer at flow rate of 0.5 ml/min.

#### 2.2.4. Gel filtration chromatography

The samples with SOD activity from the previous step were pooled and concentrated by ultrafiltration system equipped with a 10 kDa cut-off membrane. This was then processed by a Sephadex G-75 gel filtration column, regulated at a flux of 0.5 ml/min. Fractions containing SOD activity were pooled, concentrated and dialyzed against deionized water for 48 h and stored at -20 °C until used.

### 2.3. SDS-PAGE electrophoresis and protein concentration

The proteins were identified by sodium dodecyl sulfate polyacrylamide gel electrophoresis using a Mini-PROTEAN electrophoretic system (BioRad). Electrophoresis was carried out at a constant current of 85 mA [14], and the gels were stained with Comassie Brilliant Blue R-250 [15]. Protein concentration was estimated by the Bradford method [16] using bovine serum albumin as standard.

### 2.4. SOD assays and protein measurement

SOD activity was determined in 50 mM Tris-HCl buffer, pH 8.2, containing 1 mM EDTA at room temperature, using 0.2 mM pyrogallol as substrate. To 50 µl of enzyme solution diluted in 2850 µl of Tris buffer, 100 µl of 0.2 mM pyrogallol was added and the inhibition of pyrogallol autoxidation to purpurogallin in Tris buffer was measured for 5 min. The rate of autoxidation inhibition was 25%. 25 µM pyrogallol was added and the inhibition of pyrogallol autoxidation to purpurogallin in Tris buffer was measured for 5 min. The rate of autoxidation inhibition was measured by monitoring the increase in absorbance at 420 nm. One unit of SOD

activity is defined as the amount of enzyme required for 50% reduction in the rate of pyrogallol autoxidation.

### 2.5. SOD characterizations

#### 2.5.1. Optimum temperature and thermal stability

The optimum temperature for enzymatic reaction was measured using 50 mM Tris-HCl buffer, pH 8.2 at a temperature range of 20–90 °C. The activity at optimal temperature was taken as 100%. To investigate the thermal stability, enzyme solution was pre-heated in 50 mM Tris-HCl buffer, pH 8.2 at 60 and 70 °C for different intervals of time, cooled on ice and the residual activity was determined under the assay conditions. The activity of enzyme solution, kept on ice, was considered as the control (100%).

#### 2.5.2. Optimal pH and pH stability

The effect of pH on the activity was evaluated by measuring pure enzyme activity in pHs of 2–12, at room temperature. The activity at optimal pH was taken as 100%.

#### 2.5.3. Identification the type of superoxide dismutase

In order to recognize Cu/Zn-SOD, Mn-SOD and Fe-SOD isozymes, gels were incubated in different solution of KCN and H<sub>2</sub>O<sub>2</sub> with the various concentrations at the usual experimental conditions. It is known that the activity of Cu/Zn-SOD is inhibited by cyanide and H<sub>2</sub>O<sub>2</sub>, while Mn-SOD is insensitive to these treatments and Fe-SOD is only sensitive to H<sub>2</sub>O<sub>2</sub> [17].

#### 2.5.4. Determination of kinetic parameters

Catalytic activity of AmSOD was investigated at different pyrogallol concentrations under assay conditions. K<sub>m</sub>, V<sub>max</sub>, K<sub>cat</sub> and K<sub>cat</sub>/K<sub>m</sub> values were determined using Michaelis–Menten plots.

#### 2.5.5. Calculation of thermodynamic parameters

The rate constants of SOD activity reaction (k<sub>cat</sub>) and inactivation (k<sub>inact</sub>) were used to calculate the activation energy according to the Arrhenius equation [18].

$$k = Ae^{-E_a/RT} \quad (1)$$

Where, k (s<sup>-1</sup>) is the rate constant at temperature T (K), A a pre-exponential factor related to steric effects and the molecular collision frequency, R the gas constant (8.314 J mol<sup>-1</sup> K<sup>-1</sup>), and E<sub>a</sub> the activation energy of the reaction. Hence, a plot of ln k as a function of 1/T gives a curve with slope of -E<sub>a</sub>/R. The thermodynamic parameters of activation were determined as follows [19]:

$$\Delta G^\# = -RT \ln\left(\frac{k_B T}{h}\right) - RT \ln k_{cat} \quad (2)$$

$$\Delta H^\# = E_a - RT \quad (3)$$

$$\Delta S^\# = (\Delta H^\# - \Delta G^\#)/T \quad (4)$$

Where, k<sub>B</sub> is the Boltzmann constant ( $1.3805 \times 10^{-23}$  J.K<sup>-1</sup>), h the Plank's constant ( $6.6256 \times 10^{-34}$  J.s), and k<sub>cat</sub>(s<sup>-1</sup>) the rate constant at T (K).

## 3. Results and discussion

### 3.1. Isolation and purification of *avicennia marina* SOD

Figs. 2a–c show the chromatographic profiles of the eluent fractions of CM-Sephadex C-50 cation-exchanges, DEAE-Sepharose anion-exchanges and Sephadex G-75 gel filtration, respectively. Proteins were precipitated when the crude enzyme was saturated to 20–85% with ammonium sulfate. The SOD activity after this step was calculated as 236106 μmol min<sup>-1</sup>. The protein precipitate was

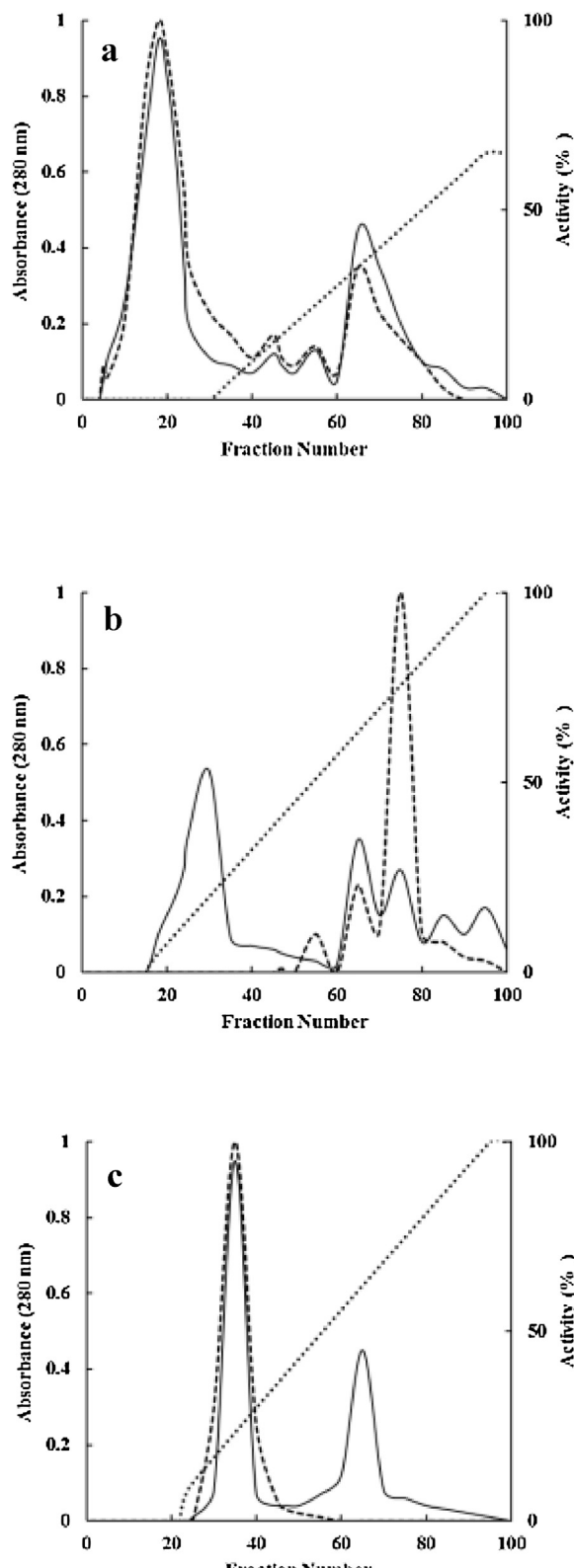


**Fig. 2.** (a–c) Chromatographic profiles of the CM-Sephadex C-50, DEAE-Sepharose and Sephadex G-75 chromatographies, respectively. Dotted line: profile protease activity; solid line: protein absorbance of the eluate.

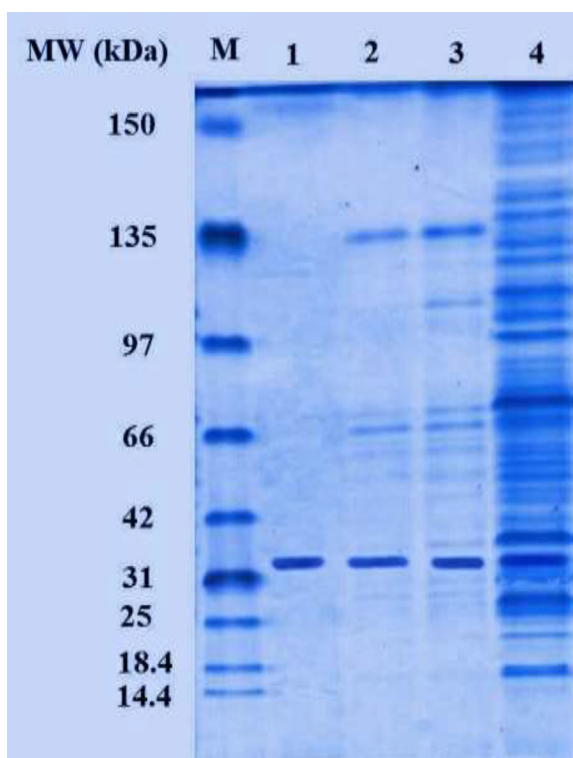


**Fig. 3.** SDS-PAGE analysis of samples obtained by the different purification steps. Proteins were detected by coomassie brilliant blue. Lane 1, crude extract; lane 2, CM-Sepharose pool; lane 3, SP-Sepharose pool; lane 4, G25 Sephadex pool. Lane M is the molecular mass marker.

then dissolved in minimal amount of 50 mM phosphate buffer pH 7.5 and dialyzed against the same buffer. The initial cation exchange chromatography with CM-Sephadex C-50 column separated SOD from most of other extracellular proteins (Fig. 2a). Chromatogram showed a small and a large protein peak. The large peak showed SOD activities with 118574  $\mu\text{M}/\text{min}$ , checked using pyrogallol as a substrate. The un-adsorbed fractions exhibiting SOD activity were pooled and applied to a DEAE-Sepharose fast flow column followed by pre-equilibration with 50 M sodium phosphate buffer at pH 7.5. In the DEAE-Sepharose anion exchange chromatography, the SOD was separated from most of other proteins with a 0–1.0 M linear gradient of NaCl (Fig. 2b). It was shown that SOD specific activity was  $315 \mu\text{mol min}^{-1} \text{mg}^{-1}$ . 13.7-fold purification was obtained after Sephadex G-75 gel filtration column with a yield of 23%, and a specific activity of  $533 \mu\text{mol min}^{-1} \text{mg}^{-1}$  (Fig. 2c). It displayed homogeneity on SDS-PAGE and migrated with a molecular mass of about 31 kDa (Fig. 3).

The results of protein content and enzyme activity obtained by each purification step are summarized in Table 1.

### 3.2. Characterizations of AmSOD

#### 3.2.1. Effect of pH on AmSOD activity

Fig. 4. shows the rate of autoxidation inhibition of pyrogallol by purified enzyme at various pH values ranging from 2 to 12. The enzyme exhibited optimum activity in a pH range of 7–9 with the maximum activity at pH 8 and a relatively high residual activity, more than 50% of the maximum, at pH 6 and 10. Wang et al. have reported an Fe-SOD from *Sonneratia alba* that is very stable in a broad range of pH, i.e. 3.5–9.5 [2]. An SOD from *Photobacterium leiognathi* was observed to be stable in the pH range of 5–11 [16]. On the other hand, it has been reported that enzyme activity was maximum in the pH range of 8.5–10 and 8–9 for *P. sepia* dismutase

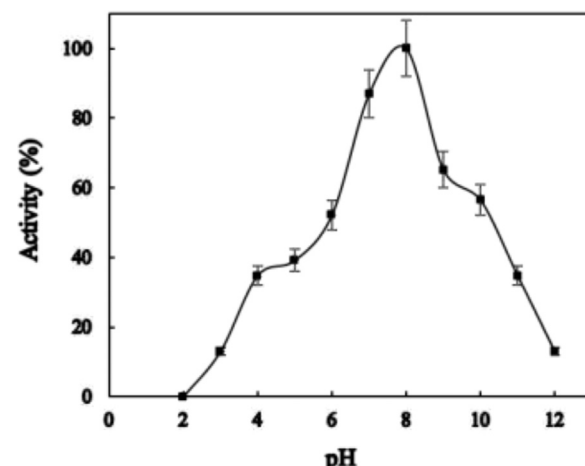


**Fig. 4.** Effect of pH on the Am SOD activity. 100% relative activity refers to the percentage of the initial reaction rate obtained by the enzyme at the pH value of maximum activity.

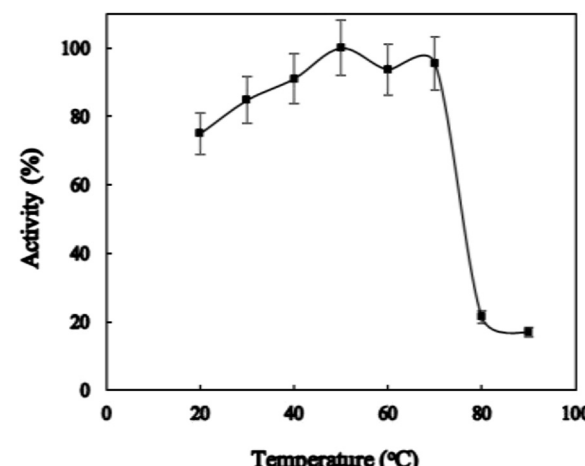


**Fig. 5.** Effect of temperature, in the range 20–90 °C, on the enzyme activity. The activity at optimal temperature was taken as 100.

tase and *P. leiognathi* dismutase, respectively [20]. A recombinant enzyme Fe/Mn-SOD from *Thallassiosira weissflogii* was inactivated in acidic pH (below 4.0), whereas it was not affected by an alkaline pH (above 9.0) [21].

#### 3.2.2. Effect of temperature on AmSOD activity

The influence of temperature on the activity of AmSOD is shown in Fig. 5. The optimal temperature for AmSOD activity was found to be in the range of 40–70 °C, showing a peak with relative activity not less than 90% when compared with other SODs in marine plants [2]. The optimal temperature for its maximal enzyme activity was 50 °C, a value similar to that has been reported for *Sonneratia alba* [2], but higher than that referred to *Enteromorpha linza* (EISOD) (35 °C) [7].

#### 3.2.3. Thermal stability of AmSOD

Enzymes are proteins, whose three dimensional structures are stabilized by weak forces. Due to their weak nature, these forces can be disrupted at high temperatures [22]. The irreversible thermoinactivation of the AmSOD was recorded in 50 mM Tris-HCl buffer, pH 8.2 at 60 °C for 50 min as shown in Fig. 6. The enzyme retained more than 85% of its activity at 60 °C, a value higher than that found for other SODs in marine organism such as *P. leiognathi*, *Gadus morhua* and *Thallassiosira weissflogii*, which showed negligible activity after incubation at 60 °C [20,21,23]. In the case of SaFe-SOD, *Lampanyc-*

**Table 1**Purification procedures of superoxide dismutase from *Avicennia marina*.

Steps of purification	Total protein (mg)	Total activity (U)	Specific activity (U/mg)	Purification fold	Yield (%)
Cell extract	9531	370520	38.9	1	100
(NH <sub>4</sub> ) <sub>2</sub> SO <sub>4</sub>	3477	236106	68.2	1.7	64
CM-Sephadex C-50	750	118574	158.1	4.0	32
DEAE-Sepharose	308	97141	315.4	8.1	26
Sephadex G-75	160	85367	533.5	13.7	23

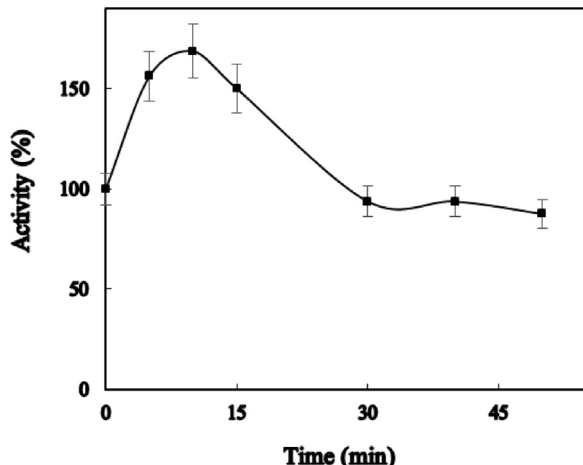


**Fig. 6.** Irreversible thermoinactivation at 70 °C (filled triangles), 80 °C (filled squares). The activity of the same enzyme solution, kept on ice, was considered as the control (100%).

*tus crocodilus* SOD and *Paralichthys olivaceus* Cu/Zn-SOD, the activity declined rapidly when the enzyme was incubated up to 70 °C for 1 h [2,24,25]. *Geobacillus* sp. EPT3 SOD retained 64 and 57% residual activity after incubation for 1 h at 80 and 90 °C, respectively [26]. Cu/Zn-SODs from *Debaryomyces hansenii* retained more than 30% of activity in 95 °C after 10 min boiling [27]. In two different allelic forms of a manganese-superoxide dismutase involved in ROS detoxification, *ApMn-SOD1* and *ApMn-SOD2*, *ApMn-SOD2* the size increased dramatically indicating the beginning of the protein denaturation/aggregation. In contrast, the size of *ApMn-SOD1* remained stable up to 74 °C and started to aggregate at about 75 °C [28].

### 3.2.4. Enzyme identification testing

The three known types of SOD are classified by their metal cofactor. Experimentally, the three types can be identified by their different sensitivities to KCN and H<sub>2</sub>O<sub>2</sub> [29]. Cu/Zn-SOD is sensitive to both; Fe-SOD is sensitive to H<sub>2</sub>O<sub>2</sub> only and Mn-SOD is resistant to both inhibitors [29,30]. In our experiments exposure to H<sub>2</sub>O<sub>2</sub>, a potent oxidant, at concentrations above 15 mM caused SOD inhibition (Fig. 7a). Low H<sub>2</sub>O<sub>2</sub> concentrations, 1–10 mM, slightly activated SOD. Since H<sub>2</sub>O<sub>2</sub> inactivates Cu/Zn-SOD and Fe-SOD but not Mn-SOD [31], the high H<sub>2</sub>O<sub>2</sub> inactivation of *AmSOD* indicated a Cu/Zn-SOD. The *AmSOD* is sensitive to KCN. Addition of 1 mM KCN to the enzyme assay showed SOD inhibition (60%), whereas 5 mM and higher levels were highly inhibitory. At a concentration of 20 mM of KCN the enzyme activity was reduced to 75% compared to the control (Fig. 7b). No SOD activity was detected at 30 mM KCN (data not shown). KCN is used as one of the SOD inhibitors and was shown to strongly inactivate Cu/Zn-SOD [29]. Based on the results, it can be suggested that our *AmSOD* could be classified as a Cu/Zn-SOD.

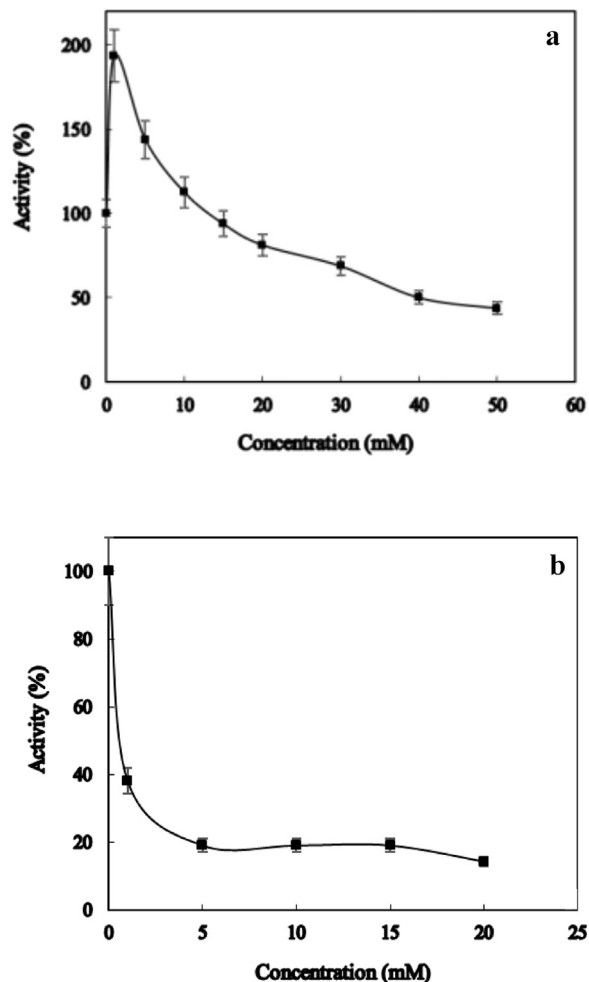


**Fig. 7.** Activity of *Am SOD* at different concentrations of H<sub>2</sub>O<sub>2</sub> (a) and KCN (b).

**Table 2**

The kinetic parameters for inhibition of pyrogallol autoxidation catalyzed by *Am SOD*. Conditions were 50 mM Tris-HCl buffer, pH 8.2, containing 1 mM EDTA at room temperature, using 0.2 mM pyrogallol as substrate. Each number is the average of at least three independent experiments.

<i>V</i> <sub>max</sub> (μM min <sup>-1</sup> )	<i>k</i> <sub>cat</sub> (s <sup>-1</sup> )	<i>K</i> <sub>M</sub> (μM)	<i>K</i> <sub>cat</sub> / <i>K</i> <sub>M</sub> (s <sup>-1</sup> μM <sup>-1</sup> )
84500	107000	11.5	9300

### 3.2.5. Kinetic and thermodynamic parameters

Proteolytic hydrolysis of pyrogallol by SOD catalysis follows the Michaelis-Menten equation. The values of *V*<sub>max</sub>, *K*<sub>M</sub>, *k*<sub>cat</sub>, and *k*<sub>cat</sub>/*K*<sub>M</sub>, measured from Lineweaver Burk plot, Table 2, were 32.9 s<sup>-1</sup>, 13.7 μM and 2.4 s<sup>-1</sup> μM<sup>-1</sup> at room temperature and pH of 8.2 respectively. The Arrhenius plot, graphed utilizing the activity values of *AmSOD* in the temperature range of 20–50 °C (data not shown), clearly suggested that beyond 50 °C the activity declined, indicating enzyme inactivation. Activation energy (*E*<sub>a</sub>) of the inhi-

**Table 3**

The thermodynamic parameters for inhibition of pyrogallol autoxidation catalyzed by *Am* SOD. Conditions were 50 mM Tris-HCl buffer, pH 8.2, containing 1 mM EDTA at room temperature, using 0.2 mM pyrogallol as substrate. Each number is the average of at least three independent experiments.

$E_a$ (kcal mol <sup>-1</sup> )	$\Delta H^\#$ (kcal mol <sup>-1</sup> )	$\Delta G^\#$ (kcal mol <sup>-1</sup> )	$\Delta S^\#$ (cal mol K <sup>-1</sup> )	$\Delta G_{E-S}^\#$ (kcal mol <sup>-1</sup> )	$\Delta G_{E-T}^\#$ (kcal mol <sup>-1</sup> )
35	34.4	3.6	103	1.4	-5.4

bition of pyrogallol autoxidation reaction catalyzed by *Am*SOD was 35 kcal mol<sup>-1</sup>K<sup>-1</sup>. The two major effects of temperature were observed on the activity of the enzyme. Firstly, an increase in the rate of the reaction at 20–50 °C, as the enzyme gained kinetic energy and, secondly, a decrease in the rate of activity due to increase in the denaturation rate of the enzyme at temperatures greater than 50 °C.

In Table 3, values of activation free energy ( $G^\#$ ), activation enthalpy ( $H^\#$ ) and activation entropy ( $S^\#$ ) for the catalytic reaction are also reported. The free activation energy of substrate binding ( $\Delta G_{E-S}^\#$ ) and the free energy for the formation of activation complex ( $\Delta G_{E-T}^\#$ ) were -1.4 and -5.4 kcal mol<sup>-1</sup>, respectively. These values confirm the great affinity of enzyme towards substrate and the following hydrolysis reaction [19].

#### 4. Conclusion

Recent advances in biotechnology, particularly in protein engineering, have provided the basis for the efficient development of enzymes with improved properties [32–42]. Antioxidant enzymes play an important role in conferring abiotic stress tolerance. Superoxide dismutase is the first enzyme in the enzymatic antioxidative pathway. Halophytic plants like mangroves have been reported to have a high level of SOD activity, having a major role in defending the mangrove species against severe abiotic stresses. In this piece of research, we have described the purification and some characteristics of Cu/Zn-SOD from Persian Gulf *Avicennia marina*. The obtained evidences from kinetic and thermodynamic parameters of the enzyme suggest that *Am*SOD can be considered as a suitable enzyme for medicinal and pharmacological applications, including therapy of fibromyalgia, diabetes, cancer, multiple sclerosis, Alzheimer's, Parkinson's disease and alcohol-induced hangover. The enzyme can also be recommended for use in preservation of biological samples such as organs for transplantation and sperms, as well as in a wide range of application for cosmetic preparations designed for skin protection.

#### References

- [1] S. Ghasemi, M. Zakaria, H. Abdul-Hamid, E. Yusof, A. Danehkar, M.N. Rajpar, A review of mangrove value and conservation strategy by local communities in Hormozgan province, Iran, J. Am. Sci. 6 (2010) 329–338.
- [2] F. Wang, Q. Wu, Z. Zhang, S. Chen, R. Zhou, Cloning, expression, and characterization of iron superoxide dismutase in *sonneratia alba*, a highly salt tolerant mangrove tree, Protein J. 32 (2013) 259–265.
- [3] K.W. Krauss, C.E. Lovelock, K.L. McKee, L. López-Hoffman, S.M. Ewe, W.P. Sousa, Environmental drivers in mangrove establishment and early development: a review, Aquat. Bot. 89 (2008) 105–127.
- [4] C. Kuenzer, A. Bluemel, S. Gebhardt, T.V. Quoc, S. Dech, Remote sensing of mangrove ecosystems: a review, Remote Sens. 3 (2011) 878–928.
- [5] U. Jabeen, A. Salim, A. Abbasi, Prediction of enzyme-inhibitor interactions in *Avicennia marina* Cu-Zn superoxide dismutase: implications of functionally significant residues in the metal binding sites, Pak. J. Biochem. Mol. Biol. 44 (2011) 1–7.
- [6] A. Bafana, S. Dutt, S. Kumar, P.S. Ahuja, Superoxide dismutase: an industrial perspective, Crit. Rev. Biotechnol. 31 (2011) 65–76.
- [7] M. Lü, R. Cai, S. Wang, Z. Liu, Y. Jiao, Y. Fang, X. Zhang, Purification and characterization of iron-cofactored superoxide dismutase from *Enteromorpha linza*, Chin. J. Oceanol. Limnol. 31 (2013) 1190–1195.
- [8] J.-K. Huang, L. Wen, H. Ma, Z.-X. Huang, C.-T. Lin, Biochemical characterization of a cambialistic superoxide dismutase isozyme from diatom *Thallassiosira weissflogii*: cloning, expression, and enzyme stability, J. Agric. Food Chem. 53 (2005) 6319–6325.
- [9] S. Prashanth, V. Sadhasivam, A. Parida, Over expression of cytosolic copper/zinc superoxide dismutase from a mangrove plant *Avicennia marina* in indica Rice var Pusa Basmati-1 confers abiotic stress tolerance, Transgenic Res. 17 (2008) 281–291.
- [10] A. Homaei, Immobilization of *Penaeus merguiensis* alkaline phosphatase on gold nanorods for heavy metal detection, Ecotoxicol. Environ. Saf. 136 (2017) 1–7.
- [11] A. Homaei, M. Ghanbarzadeh, F. Monsef, Biochemical features and kinetic properties of  $\alpha$ -amylases from marine organisms, Int. J. Biol. Macromol. 83 (2016) 306–314.
- [12] A. Homaei, F. Lavajoo, R. Sariri, Development of marine biotechnology as a resource for novel proteases and their role in modern biotechnology, Int. J. Biol. Macromol. 88 (2016) 542–552.
- [13] S. Sharifian, A. Homaei, R. Hemmati, K. Khajeh, Light emission miracle in the sea and preeminent applications of bioluminescence in recent new biotechnology, J. Photochem. Photobiol. B 172 (2017) 115–128.
- [14] U.K. Laemmli, Cleavage of structural proteins during the assembly of the head of bacteriophage T4, nature 227 (1970) 680–685.
- [15] C.M. Wilson, Staining of proteins on gels: comparisons of dyes and procedures, Methods Enzymol. 91 (1983) 236–247.
- [16] M.M. Bradford, A rapid and sensitive method for the quantitation of microgram quantities of protein utilizing the principle of protein-dye binding, Anal. Biochem. 72 (1976) 248–254.
- [17] O. Hammouda, Purification and identification of the type of superoxide dismutase from *Gloeocapsa* sp., Folia Microbiol. 44 (1999) 32–36.
- [18] S. Arrhenius, On the reaction velocity of the inversion of cane sugar by acids, J. Phys. Chem. 4 (1889) 226.
- [19] A. Homaei, Purification and biochemical properties of highly efficient alkaline phosphatase from *Fenneropenaeus merguiensis* brain, J. Mol. Catal. B: Enzym. 118 (2015) 16–22.
- [20] K. Puget, A. Michelson, Iron containing superoxide dismutases from luminous bacteria, Biochimie 56 (1974) 1255–1267.
- [21] C.-F. Ken, T.-M. Hsiung, Z.-X. Huang, R.-H. Juang, C.-T. Lin, Characterization of Fe/Mn-superoxide dismutase from diatom *Thallassiosira weissflogii*: cloning, expression, and property, J. Agric. Food Chem. 53 (2005) 1470–1474.
- [22] A.A. Homaei, A.B. Mymandi, R. Sariri, E. Kamrani, R. Stevanato, S.-M. Etezad, K. Khajeh, Purification and characterization of a novel thermostable luciferase from *Benthosema pterotum*, J. Photochem. Photobiol. B 125 (2013) 131–136.
- [23] A. Bartkowiak, E. Grzelinska, I. Varga, W. Leyko, Studies on superoxide dismutase from cod (*Gadus morhua*) liver, Int. J. Biochem. 13 (1981) 1039–1042.
- [24] K. Osatomí, Y. Masuda, K. Hara, T. Ishihara, Purification, N-terminal amino acid sequence, and some properties of Cu, Zn-superoxide dismutase from Japanese flounder (*Paralichthys olivaceus*) hepatopancreas, Comp. Biochem. Physiol. B: Biochem. Mol. Biol. 128 (2001) 751–760.
- [25] C. Capo, M.E. Stroppolo, A. Galtieri, A. Lanía, S. Costanzo, R. Petruzzelli, L. Calabrese, F. Politicelli, A. Desideri, Characterization of Cu, Zn superoxide dismutase from the bathypelagic fish *Lampanyctus crocodilus*, Comp. Biochem. Physiol. B: Biochem. Mol. Biol. 117 (1997) 403–407.
- [26] Y. Zhu, G. Wang, H. Ni, A. Xiao, H. Cai, Cloning and characterization of a new manganese superoxide dismutase from deep-sea thermophilic *Geobacillus* sp. EPT3, World J. Microbiol. Biotechnol. 30 (2014) 1347–1357.
- [27] N. Hernandez-Saavedra, J. Ochoa, Copper-zinc superoxide dismutase from the marine yeast *Debaryomyces hansenii*, Yeast 15 (1999) 657–668.
- [28] M. Bruneaux, J. Mary, M. Verheyen, O. Lecompte, O. Poch, D. Jollivet, A. Tanguy, Detection and characterisation of mutations responsible for allele-specific protein thermostabilities at the Mn-Superoxide dismutase gene in the deep-Sea hydrothermal vent polychaete *alvinella pompejana*, J. Mol. Evol. 76 (2013) 295–310.
- [29] C. Bowler, M.V. Montagu, D. Inze, Superoxide dismutase and stress tolerance, Annu. Rev. Plant Biol. 43 (1992) 83–116.
- [30] F. Zeinali, A. Homaei, E. Kamrani, Sources of marine superoxide dismutases: characteristics and applications, Int. J. Biol. Macromol. (2015).
- [31] S. Kanematsu, K. Asada, CuZn-superoxide dismutases from the fern *Equisetum arvense* and the green alga *Spirogyra* sp.: occurrence of chloroplast and cytosol types of enzyme, Plant Cell Physiol. 30 (1989) 717–727.
- [32] A. Homaei, Enzyme immobilization and its application in the food industry, Adv. Food Biotechnol. (2015) 145.
- [33] A. Homaei, Enhanced activity and stability of papain immobilized on CNBr-activated sepharose, Int. J. Biol. Macromol. 75 (2015) 373–377.
- [34] A. Homaei, H. Barkheh, R. Sariri, R. Stevanato, Immobilized papain on gold nanorods as heterogeneous biocatalysts, Amino Acids 46 (2014) 1649–1657.
- [35] A. Homaei, R. Etemadipour, Improving the activity and stability of actinidin by immobilization on gold nanorods, Int. J. Biol. Macromol. 72 (2015) 1176–1181.
- [36] A. Homaei, D. Saberi, Immobilization of  $\alpha$ -amylase on gold nanorods: an ideal system for starch processing, Process Biochem. 50 (2015) 1394–1399.
- [37] A. Homaei, F. Samari, Investigation of activity and stability of papain by adsorption on multi-wall carbon nanotubes, Int. J. Biol. Macromol. 105 (2017) 1630–1635.

- [38] A. Homaei, R. Stevanato, R. Etemadipour, R. Hemmati, Purification catalytic, kinetic and thermodynamic characteristics of a novel ficin from *Ficus johannis*, *Biocatal. Agric. Biotechnol.* 10 (2017) 360–366.
- [39] A.A. Homaei, R.H. Sajedi, R. Sariri, S. Seyfzadeh, R. Stevanato, Cysteine enhances activity and stability of immobilized papain, *Amino Acids* 38 (2010) 937–942.
- [40] A.A. Homaei, R. Sariri, F. Vianello, R. Stevanato, Enzyme immobilization: an update, *J. Chem. Biol.* 6 (2013) 185–205.
- [41] S. Rouzbahan, S. Moein, A. Homaei, Total antioxidant capacities and reduction of ferric ions by extracts of three medicinal plants and their fractions, *Bimon. J. Hormozgan Univ. Med. Sci.* 20 (2016) 245–254.
- [42] S. Rouzbahan, S. Moein, A. Homaei, M.R. Moein, Kinetics of  $\alpha$ -glucosidase inhibition by different fractions of three species of Labiate extracts: a new diabetes treatment model, *Pharm. Biol.* 55 (2017) 1483–1488.